Available online at www.sciencedirect.com

SCIENCE DIRECT®

Earth and Planetary Science Letters 235 (2005) 741–751

EPSL

www.elsevier.com/locate/epsl

Reconstruction of temperature in the Central Alps during the past 2000 yr from a $\delta^{18}O$ stalagmite record

A. Mangini[a,*], C. Spötl[b], P. Verdes[a]

[a] *Forschungsstelle Radiometrie, Heidelberger Akademie der Wissenschaften, Im Neuenheimer Feld 229, 69120 Heidelberg, Germany*
[b] *Institut für Geologie und Paläontologie, Leopold-Franzens-Universität Innsbruck, Innrain 52, 6020 Innsbruck, Austria*

Received 3 September 2004; received in revised form 10 May 2005; accepted 12 May 2005
Available online 17 June 2005
Editor: E. Bard

Abstract

The precisely dated isotopic composition of a stalagmite from Spannagel Cave in the Central Alps is translated into a highly resolved record of temperature at high elevation during the past 2000 yr. Temperature maxima during the Medieval Warm Period between 800 and 1300 AD are in average about 1.7 °C higher than the minima in the Little Ice Age and similar to present-day values. The high correlation of this record to $\Delta^{14}C$ suggests that solar variability was a major driver of climate in Central Europe during the past 2 millennia.

Keywords: Medieval Warm Period; temperature; Central Alps; stalagmite record; Holocene; stable isotopes

1. Introduction

The knowledge of the evolution of temperature during the last 2000 yr (directly measured data are available only for the last 200 yr) is important as climate models are often verified to this curve. The temperature reconstruction by the IPCC is utilized in the majority of cases for verification [1,2]. This reconstruction is mainly based on data from tree rings, as well as from high latitude ice cores, corals and sea-surface temperature from highly resolved near-shore sediments. This temperature curve only shows small variations during the last 1800 yr, but demonstrates an abrupt temperature increase after 1860, which is generally ascribed to the increase of the greenhouse gases CO_2 and CH_4 in the atmosphere. However, it is presently being discussed what type of climate existed during Medieval times [3] and if the Medieval Warm Period (MWP) was a global or regional phenomena [4]. The statistical uncertainty in the IPCC curve in the section around 1000 AD is about ±0.5 °C [1]. However, another major source of uncertainty is that biological samples, which are the foundation of climate reconstructions, tend to accommodate with climate change, and the accuracy of the temperature estimates based on biological proxies is not likely to be better

* Corresponding author.
E-mail address: augusto.mangini@iup.uni-heidelberg.de (A. Mangini).

0012-821X/$ - see front matter © 2005 Elsevier B.V. All rights reserved.
doi:10.1016/j.epsl.2005.05.010

than 1.3 °C [5]. Several other climate archives, such as ice cores [6], sediments from high accumulation sites [7] or mountain glaciers in the Alps [8], suggest that the Northern Hemisphere has undergone major climatic changes during the last 2000 yr. The Roman Period about 2000 yr before present as well as the MWP, lasting from about 800 to 1300 AD were recognized as phases of glacier retreat, whereas the Little Ice Age (LIA), from about 1400 to 1850 AD, marked a period of generally positive glacier mass balances [9]. Recently, Moberg et al. [10] have reconstructed temperatures for the Northern Hemisphere from low and high resolution proxy data from eleven archives. Their multi-proxy reconstruction reveals a relatively large multicentennial variability which clearly contrasts the reconstructions which have mainly used tree-ring data sets of annual and decadal resolution [1]. The amplitude of temperature variations between the LIA and the MWP in their stack is about 0.9 °C.

Because of this ongoing discussion, more climate records are required to explain the likely causes of climate variations over the last two millennia. Here we reconstruct the evolution of temperature in the Central Alps during the last 2000 yr from the $\delta^{18}O$ record of a well-dated stalagmite, SPA 12, retrieved from a high-alpine cave site. Our reconstruction relies on the temperature dependence of processes in the atmosphere that are recorded during the carbonate formation.

1.1. Description of the sample and results

The stalagmite SPA 12 was retrieved from Spannagel Cave, which is part of a high-elevation cave system in the Central Alps of Austria [11]. The cave's entrance is located at 2524 m a.s.l. and the site at which SPA 12 formed is located at 2347 m a.s.l. The stalagmite formed in a remote part of the 10 km long cave system where today's air temperature is constant at +1.8 °C and relative humidity is near condensation throughout the year. When SPA 12 was removed in 1998, its top was wet, but the dripping rate from the stalactite above was extremely slow. The sample is composed of white, densely crystalline low-Mg calcite, showing columnar-shape crystals in thin section.

13 ages were derived from the 20 cm long stalagmite applying the Th/U method (TIMS) as described earlier [12,13]. Dating is possible at high precision due to high uranium content. The age–depth relationship reveals a fairly constant growth rate of 75 μm/yr during the last 2000 yr and a slower rate of 17 μm/yr in the section between 2000 and 5000 yr at the base of the sample (Fig. 1A). The youngest age at 0.2 cm is 64 ± 4 yr, and a linear fit through the top 5 points suggests that the age at the top of stalagmite has an approximate date of 1950 AD (Table 1). Applying a growth rate model we converted the depth profile into an age profile (Fig. 1b). In this study we only discuss the sections with better time resolution deposited over the last 2000 yr. The $\delta^{18}O$ age profile consists of 700 samples obtained at 100 μm increments (using micromilling, for analytical details see [14]) thus resulting in an average resolution of slightly over one year per isotope sample. Values vary between −8.2‰ and −6.8‰ (VDPB). The $\delta^{18}O$ values of −7.5‰ from the top of the stalagmite are similar to calcite recently deposited in the cave at −7.8‰ in equilibrium with modern drip water of -11.3 ± 0.2 ‰ (VSMOW) at today's cave temperature of +1.8 °C. The isotopic composition of calcite depends on (i) the isotopic composition of precipitation, (ii) kinetic effects, leading to simultaneous enrichments of heavier isotopes in the calcite and a correlation between $\delta^{13}C$ and $\delta^{18}O$, and (iii) temperature with a gradient of −0.22‰/°C. The $\delta^{13}C$ profile shows no correlation with $\delta^{18}O$ in any of the section profiles, suggesting that kinetic effects played a minor role during stalagmite growth at this location. As we exclude kinetic effects, the changes in the isotopic composition of the calcite only depend on the variation in precipitation and temperature during calcite formation [15,16].

1.2. Derivation of the temperature record for the past 2000 yr

The conversion of the isotopic profile into temperature is performed by applying the transfer function shown in Fig. 2. This curve is obtained from 5 points with known temperature from the average yearly temperature reconstruction for the Alps by Luterbacher et al. [17] and the isotopic composition of the stalagmite in the corresponding sections. The uppermost point marks the present-day conditions in Spannagel at +1.8 °C and $\delta^{18}O = -7.8$‰. The average temperature in the Alps during the coldest period between 1688 and 1698 coincided with the Maunder Minimum. As de-

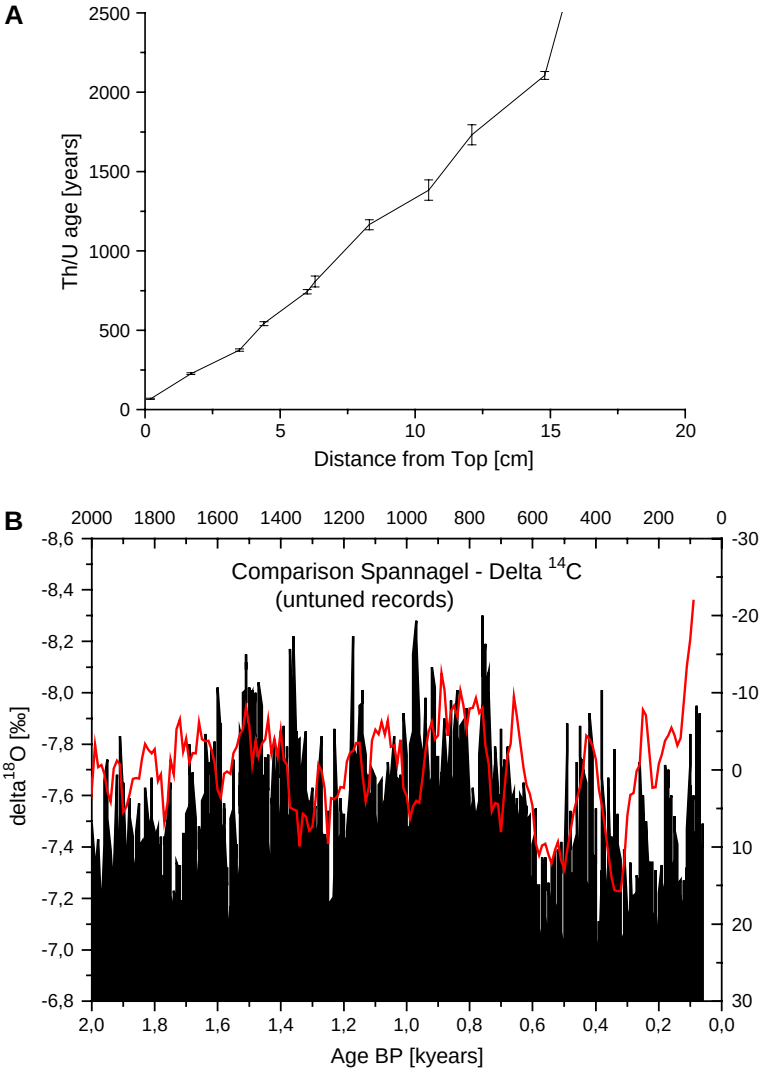

Fig. 1. (A) The age depth relationship of SPA 12 (two sigma errors of dating). (B) The profile of $\delta^{18}O$ in SPA 12 against age together with the $\Delta^{14}C$ record derived from tree rings (untuned records). Periods of lighter isotopes coincide with lower $\Delta^{14}C$ concentration in the atmosphere [30].

rived from Luterbacher's data, the average temperature in this period was -1.0 (± 0.5) °C, about 1.8 °C lower than in the period between 1995 and 1998. The section of the stalagmite that grew during this period has the heaviest $\delta^{18}O$ values in the profile (-6.99 ± 0.14‰). This cold period delivers the second temperature point on the calibration curve. We choose as third and lowest point on the calibration curve the lowest isotopic values of calcite ($\delta^{18}O = -6.8$‰), which we assume to be deposited close or slightly below 0 °C, as stalagmite growth will cease when temperature falls below the freezing point. We ascribe an uncertainty of 0.2 °C to this point.

The reconstruction of temperature is corroborated by two further points on the transfer function. The average temperature in the Alps in the period between AD 1800 and 1890 was about 1.15 ± 0.50 °C lower than in the period between 1995 and 1998. Thus, Luterbacher's reconstruction suggests that then the temperature in the Alps was slightly lower than the

Table 1
Results of Th- and U-analyses on SPA 12

Lab. nr.	δU	Error	^{238}U	Error	232Th	Error	^{230}Th	Error	Age (corr.)	Error	Age (uncorr.)	Depth
	(‰)	(abso.)	(ug/g)	(abso.)	(ng/g)	(abso.)	(pg/g)	(abso.)	(ka)	(ka)	(ka)	(cm)
1615	16.3	2.9	10.798	0.022	2.364	0.010	0.1136	0.0068	0.064	0.004	0.070	0.2 ± 0.2
2132	27.8	4.6	13.863	0.035	0.5755	0.0027	0.491	0.011	0.230	0.005	0.231	1.5 ± 0.2
2133	16.1	2.8	13.635	0.026	1.1384	0.0052	0.793	0.015	0.382	0.008	0.384	3.4 ± 0.2
3405	13.7	1.4	13.669	0.014	0.9100	0.0067	1.139	0.024	0.548	0.012	0.550	4.8 ± 0.1
3406	14.1	1.5	8.8274	0.0088	1.952	0.011	1.013	0.018	0.751	0.014	0.758	6.0 ± 0.1
2101	25.5	2.9	10.180	0.022	4.328	0.038	1.846	0.052	1.179	0.033	1.191	8.0 ± 0.2
1935	14.0	7.7	10.187	0.014	1.411	0.096	2.17	0.10	1.401	0.064	1.411	10.0 ± 0.2
2102	22.2	3.0	10.891	0.025	8.76	0.11	2.920	0.073	1.749	0.044	1.772	12.0 ± 0.2
1616	24.5	3.3	11.3246	0.0260	1.459	0.0054	3.70	0.04	2.154	0.026	2.157	14.7 ± 0.2
1972	11.0	6.5	8.407	0.019	<0.1	–	4.274	0.060	3.392	0.050	3.392	16.2 ± 0.2
1936	4.9	6.9	6.9216	0.0083	0.158	0.037	4.457	0.053	4.348	0.060	4.366	18.0 ± 02
1973	8.7	6.8	10.852	0.016	0.694	0.030	8.15	0.14	5.043	0.090	5.078	20.3 ± 0.2
1374	16.0	3.7	10.066	0.017	3.018	0.028	7.45	0.42	4.94	0.27	4.98	22.0 ± 0.2

0.7 °C lower global temperature as reported in the IPCC curve [2]. This temperature, together with the average of the $\delta^{18}O$ value of -7.35 ± 0.18‰ in the section corresponding to the interval 1800–1890, yields the fourth point on the curve. The fifth point at $\delta^{18}O$ -7.5 ± 0.1‰ at the top of the stalagmite corresponds to the calcite deposited around AD 1950 when temperature was 0.3 ± 0.3 °C lower than today, a period when there was positive glacier growth in the Alps.

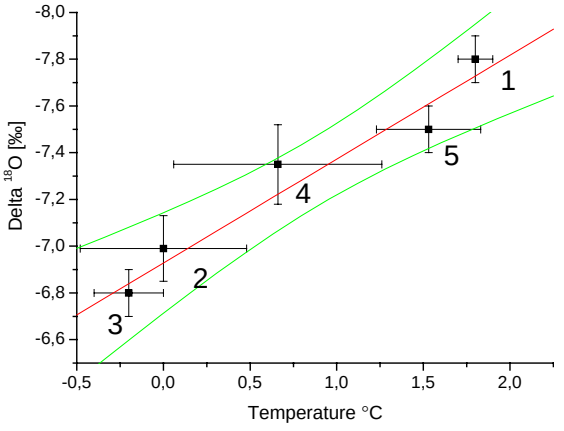

Fig. 2. The red curve shows the development of $\delta^{18}O$ as a function of temperature observed in SPA 12. The curve was reconstructed from five points with known temperature in the Alps derived from the reconstruction of [17] and their corresponding $\delta^{18}O$ values in SPA 12. Also plotted are the upper and lower 95% confidence limits. (For interpretation of the references to colour in this figure legend, the reader is referred to the web version of this article.)

The transfer function has a slope of −0.44‰/°C and the net slope corrected for the temperature effect of deposition of calcite at equilibrium is −0.22‰/°C (−0.44‰/°C+0.22‰/°C).

We ascribe the observed net slope of isotopic composition as a result of a variable mixing of the heavier summer and lighter winter precipitation.

Based on this transfer function, temperature reconstructed from the isotopic record ranges between 0 °C and 2.7 °C (Figs. 3 and 4). Considering the confidence limits of the calibration curve, the uncertainty of our

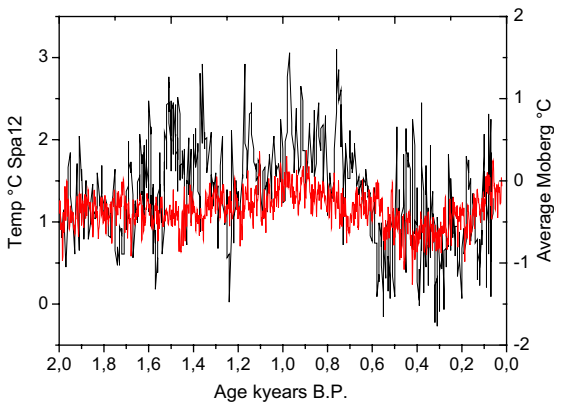

Fig. 3. Comparison of the temperature derived from SPA 12 (black curve) with the average stack for the N.H. by Moberg et al. (red curve). As expected SPA 12 shows a larger amplitude (about 2.7 °C) than the stack for the N.H (0.9 °C). (For interpretation of the references to colour in this figure legend, the reader is referred to the web version of this article.)

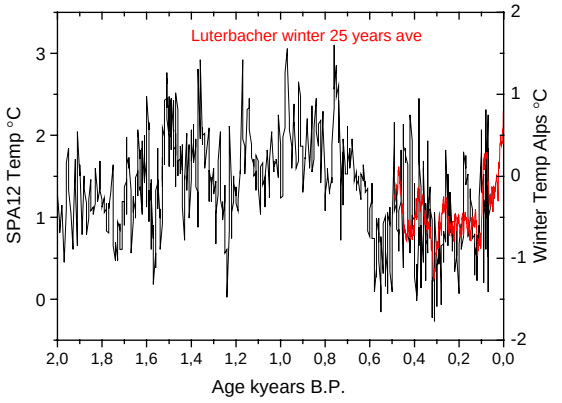

Fig. 4. Comparison of the temperature derived in SPA 12 with the yearly winter temperature in the Alps as derived by Luterbacher et al.

temperature reconstruction for Spannagel is about ±0.3 °C. We observe the lowest values in the section formed during the Little Ice Age (AD 1400–1850), and maximum values in the section corresponding to the MWP (approx. AD 800–1300). These latter values are even slightly higher than those of the top section of the stalagmite (1950 AD) and higher than the present-day temperature of 1.8 °C.

We cannot exclude that there have been some periods when stalagmite growth stopped in the past, for example if the temperature in the cave went significantly below 0 °C. However, the record of Luterbacher et al. indicates that the Maunder Minimum was one of the coldest periods during the last 500 yr and that colder events were short lasting and infrequent. Therefore we claim that if any hiatus occurred it did not distort significantly our age reconstruction of SPA 12. Furthermore, the high number of precise Th/U-ages reduces this uncertainty anyway.

The temperature reconstruction from SPA 12 shows a pattern similar to other climatic archives from the Northern Hemisphere including Greenland ice cores, sea-surface temperatures (SST) from the Bermuda Rise, as well as to the reconstruction of glacier tongue advances and retreats in the Alps (Fig. 5) [9,8,7,18]. There is a good correspondence to the reconstruction of SST at Bermuda Rise (Figs. 5 and 6) showing a temperature difference of about 2 °C between the MWP and LIA [7,19]. However, the range of relative temperature variations in SPA 12 of about 2.7 °C exceeds that of the ice cores, where ΔT between the LIA minima and MWP maximum is approximately 1.5 °C.

Comparison with the multi-proxy reconstruction by Moberg et al. is shown on Fig. 3.

Both curves depict the maximum of temperature in the N.H. during the MWP. As expected the multi-proxy stack has smaller amplitude of about 0.9 °C than our curve from Spannagel between the minimum in the LIA and the MWP events. The smaller amplitude is obvious, since Moberg's reconstruction, resulting from a stack of several different archives with independent age control, looses amplitude as a consequence of the uncertainty in the ages of the single curves. In contrast, the temperature record from SPA 12 with an extremely good age control and with a better than decadal resolution of ^{18}O, gives insight into temperature variations that were not recorded in other archives.

Overall, the good correlation of our reconstruction of temperature from SPA 12 with other archives supports their conclusions. Together, these non-faunal archives indicate that the MWP was a climatically distinct period in the Northern Hemisphere. This conclusion is in strong contradiction to the temperature reconstruction by the IPCC, which only sees the last 100 yr as a period of increased temperature during the last 2000 yr.

The high resolution record from SPA 12 has a number of interesting features:

a) During the MWP we observe periods lasting between 20–50 yr with temperatures higher than the average over the last 2000 yr. One may speculate that these warmer periods are related to the strength of ocean circulation [20] or to changes in the extension of the ice cover of the N. Atlantic Ocean [21], but more data are needed to confirm this conclusion.
b) The temperature derived from SPA 12 compares better to Luterbacher's reconstruction of the winter temperature than to their yearly average temperature in the Alps (Fig. 4).
c) We observe a high correlation between $\delta^{18}O$ (and temperature) and $\Delta^{14}C$, that reflects the amount of radiocarbon in the upper atmosphere. In Fig. 1 the non-tuned records are shown. The profile of $\delta^{18}O$ was tuned to the tree-ring calibrated profile of $\Delta^{14}C$, similarly as done earlier for several other

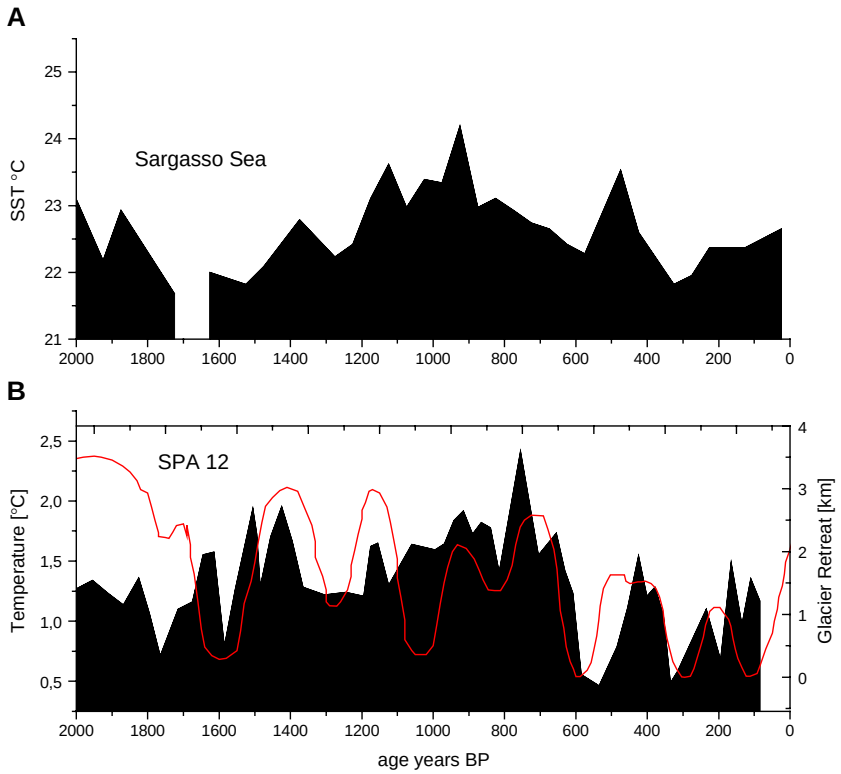

Fig. 5. Comparison to other climate archives: (A) sea level temperatures derived from $\delta^{18}O$ in foraminifera, (B) SPA 12, the red curve is the retreat of the Great Aletsch Glacier in the Alps. The resolution of SPA 12 was smoothed to a resolution comparable to that of the sediment shown in (A). We have shifted the time scale of the curve of the Aletsch Glacier by 50 yr (towards older ages). (For interpretation of the references to colour in this figure legend, the reader is referred to the web version of this article.)

stalagmites [13,22,23]. Tuning delivers a high correlation between $\delta^{18}O$ in SPA 12 and $\Delta^{14}C$ ($r=0.61$) (Figs. 7 and 8). The maxima of $\delta^{18}O$ coincide with solar minima (Dalton, Maunder, Sporer, Wolf, as well as with minima at around AD 700, 500 and 300). This correlation indicates that the variability of $\delta^{18}O$ is driven by solar changes, in agreement with previous results on Holocene stalagmites from Oman, and from Central Germany [13,22,23]. In stalagmites from N. W. Germany we have found that periodic drier sequences correlate with periods of increased $\Delta^{14}C$ throughout the last part of the Holocene [22], corroborating the findings of Bond et al. in the North Atlantic [20]. In the Appendix we derive the variance explained by solar forcing and by CO_2 for SPA 12 with two different models and compare them with values derived for the stack by Moberg and for the temperature curve by Mann and Jones.

1.3. The relationship between temperature and the isotopic composition of carbonate at Spannagel

The fact that we are able to determine a relationship between temperature and the isotopic composition of carbonate at Spannagel is certainly unusual, as for most stalagmites the kinetic effect and the source effects overprint the temperature signal. The main reason is that SPA 12 displays a negligible kinetic effect, probably due to the very low temperature in the cave which reduces the outgassing of excess CO_2, accompanied by high drip rates during the summer. Consequently, the relationship between temperature and isotopic composition results from a mixing of different types of precipitation that varies with temperature. The isotopic composition of precipitation in Europe strongly depends on the amount of rainout of the clouds; on its path across the continent and as temperature decreases, precipitation becomes lighter.

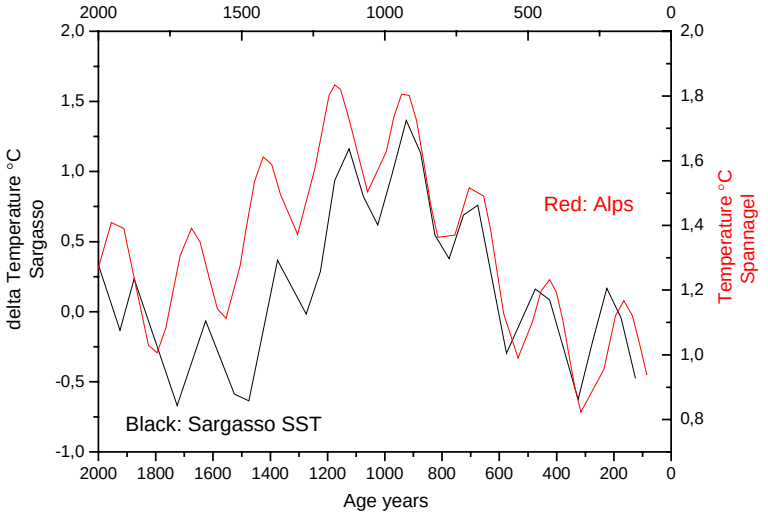

Fig. 6. The comparison of the temperature in SPA 12 (smoothed curve) with the SST curve from the Bermuda Rise was performed applying the method described by Loehle [19]. The curves of temperature from the Bermuda Rise and from SPA 12 show deviations from the 1874 and 1915 values, respectively. They are approximated by a function with a linear term and a sum of three cyclic terms, where the fits were performed without any constraints (model 3 of Loehle). Independent fits of both SST and SPA 12 show a very similar run during the last 2000 yr.

Winter precipitation is significantly lighter than that in summer and precipitation that falls upon Central Europe is more depleted than that from the southern trajectories which partly pass over the Mediterranean Sea (yearly average Stuttgart: −8.1‰, Genoa: −5.6‰ [24].

A first explanation for the observed relationship between isotopic composition and temperature is that the trend at Spannagel relies on a response of hydrology to climate, for example if the supply of winter precipitation to the ground water reservoir feeding the drip water is reduced during periods of

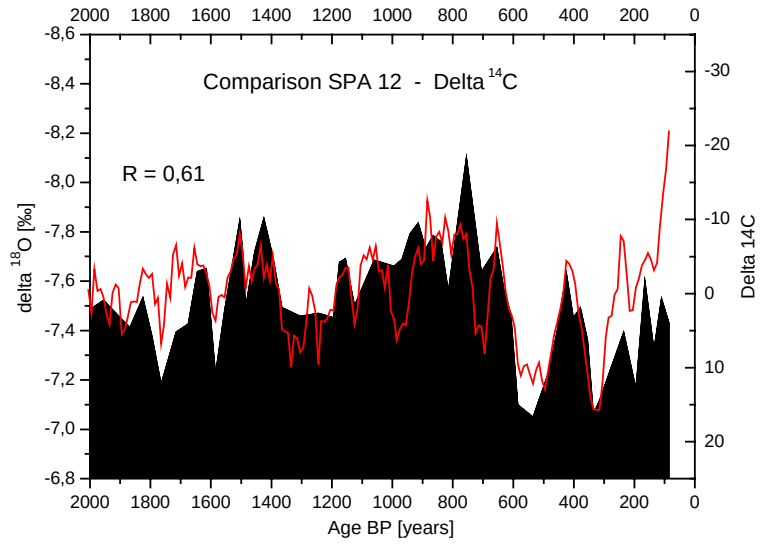

Fig. 7. $\delta^{18}O$ record of SPA 12 (from Fig. 1, smoothed) tuned to $\Delta^{14}C$ ($r=0.61$), the red curve shows the plot of residual $\Delta^{14}C$, which is assumed to be a function of the intensity of solar irradiation. (For interpretation of the references to colour in this figure legend, the reader is referred to the web version of this article.)

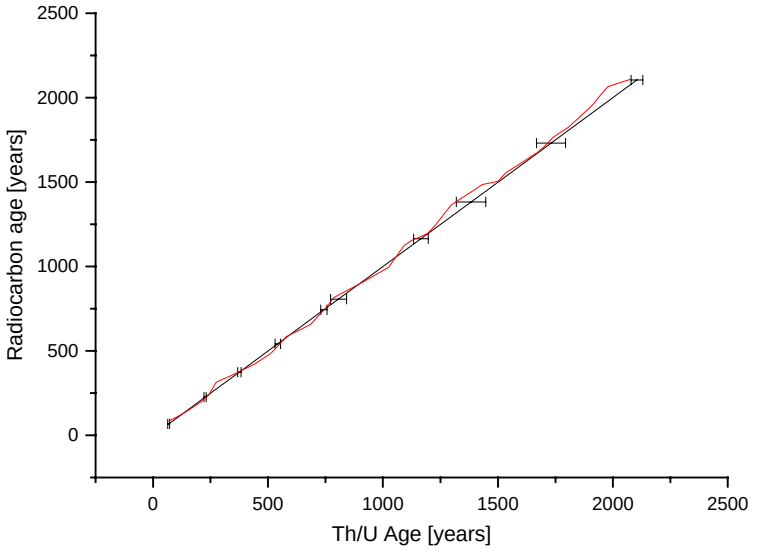

Fig. 8. Deviation of Th/U-ages from the "true" ^{14}C ages required to obtain the correlation between the $\Delta^{14}C$ and $\delta^{18}O$ profile in SPA 12 shown Fig. 7.

colder climate. The drip water isotope data suggest that presently winter precipitation contributes about 40% to the drip water that forms stalagmites. A reduction of the winter contribution to 32% would generate 1‰ heavier drip water. Removal of snow on the ridge above the karst system by wind erosion or a shorter lasting melting period in summer reducing the supply of winter precipitation to the aquifer are possible explanations that are being presently tested.

Another possible explanation is that the isotopic composition of stalagmites in Spannagel reflects changes of the temperature and the strength of the NAO index. In Northern Europe, periods of low NAO index are characterized by colder and drier winters with reduced contribution of precipitation originating from the North Atlantic [25,26]. The opposite mode, a high NAO index, causes wet and warmer winters in Northern Europe. Temperature correlates with the NAO both in Central Europe and in the Alps, whereas it anticorrelates with the NAO in southern Europe [27,25]. Wanner et al. have shown this relationship to have existed since 1700 when meteorological records were first available, although the correlation of temperature to the NAO index at times breaks down.

For a composite of seven stations in Austria, Kaiser et al. [28] have shown that the isotopic composition of precipitation correlates with the NAO index and that a positive NAO index is accompanied by $\delta^{18}O$ values 1–2‰ heavier than average. This trend may be ascribed to a reduction of the share of lighter winter precipitation during NAO^{+}, resulting in a heavier yearly average precipitation. They also conclude that two localities in Austria, Villacher Alpe and Graz, receive a significant contribution of heavier Mediterranean winter precipitation [28]. A similar situation may arise at Spannagel, where data from regular monitoring of drip water at different locations conducted since 1998 show that drip water is heavier by about 2 ‰ in comparison to the regional $\delta^{18}O_{ppt}$ vs. the altitude trend in the Austrian Alps [29]. This second hypothesis, that could explain the relationship between temperature and isotopic composition in Spannagel, assumes that the cave receives variable amounts of precipitation from northern and southern sources. If so, it becomes sensitive to variations of the NAO index: during high NAO index annual precipitation at Spannagel becomes lighter due to a larger contribution of precipitation from northern trajectories, and vice versa. This behavior is opposite to the trend of isotopic composition of precipitation in Austria, where heavier isotopic composition is related to a positive NAO, as described by Kaiser et al. [28]. Therefore, if this second hypothesis is correct, it requires that the source-effect at Spannagel Cave overcompensates the

Table 2
Variance of temperature reconstructions explained by solar forcing and CO_2 in linear models

	$E.V._{Sun}$	$E.V._{CO_2}$
SPA 12	0.279	0.001
[10]	0.147	0.058
[2]	0.092	0.009

winter/summer-effect, leading to observed heavier precipitation with colder temperatures.

Both these hypotheses will be tested in the future. Recapitulating, despite that the process is not yet well understood, the good correlation of the temperature in Spannagel both with the winter temperature in the Alps as well as with ^{14}C, clearly suggests that the intensity of the sun plays a mayor role on the isotopic composition of the drip water in the cave. In the first hypothesis, it would explain the variability of hydrology, in the second, it would rather suggest that the sources of precipitation vary in accordance with the solar intensity.

2. Conclusions

Stalagmite SPA 12 from the Alps yields a highly resolved record of changes in climate at high elevation in Central Europe during the past 2000 yr at a resolution comparable to that of the Northern Hemisphere ice core records. The similarity between records in Europe, Greenland and from the Bermuda Rise suggests that the MWP had a major impact on the Northern Hemisphere climate. The temperature difference between the LIA and the MWP is about 1.7 °C on average. This difference is in good agreement with those derived from sediment cores from the Bermuda Rise but is larger than the reconstruction of temperature for the Northern Hemisphere from low frequency stacks and significantly larger than that in the IPCC report. The highly significant correlation with $\Delta^{14}C$ underlines the important role of solar forcing as a driver of Northern Hemisphere climate during the past 2 millennia.

Acknowledgements

We thank M. Wimmer and R. Eichstädter for their work in the stable isotope and TIMS laboratories, and E. Wiedner and J. Ilmberger for interesting discussions. The manuscript was improved by thoughtful reviews by S. Frisia, G. Hoffmann and an anonymous reviewer. The funding was supplied by the DEKLIM program, the Austrian Science Funds (Y122-GEO) and the Alexander von Humboldt Foundation (P.V.).

Appendix A. Explained variances

In this Appendix we study the amount of variance in SPA 12 explained by solar forcing and CO_2 over the last 2000 yr. To this end we considered both a linear and a nonlinear framework, as described below. For comparison, we also include a similar analysis on the temperature reconstructions by [10,2].

To measure to which extent solar forcing ([30]) and CO_2 ([31]) contribute to variance production in SPA 12, we first followed the standard practice of assuming that the observations of interest can be explained as a linear combination of the candidate signals. If R_x denotes the cross-correlation coefficient between (non-tuned) SPA 12 and variable X, then the variance explained by X (denoted hereafter $E.V._X$) is simply given by R_x^2. In this linear regression setting we obtain the results reported in Table 2.

A few comments are in order at this point. First, to understand the surprisingly low fraction of variance explained by CO_2, we recall that in this study we have not employed sliding windows of a decadal scale but the whole history of the last 2000 yr. The flat evolution of CO_2 during the first 19 centuries yields almost vanishing correlation coefficients with the temperature reconstructions, even for [2]. Second, a comparison among the results for $E.V._{Sun}$ in Table 2 confirms our previous observation that SPA 12 follows more closely the solar signal.

We have also explored a nonlinear regression framework, using artificial neural networks (ANNs)

Table 3
Variance explained by linear and nonlinear models when modeling temperature using both solar and CO_2 inputs

	$E.V._{LinearRegression}$	$E.V._{ANN}$
SPA 12	0.28 ± 0.07	0.60 ± 0.05
[10]	0.18 ± 0.08	0.39 ± 0.07
[2]	0.12 ± 0.06	0.30 ± 0.07

Table 4
Variance explained by solar forcing and CO_2 in nonlinear models

	$E.V._{Sun}$	$E.V._{CO_2}$
SPA 12	0.40 ± 0.08	0.29 ± 0.07
[10]	0.23 ± 0.07	0.12 ± 0.05
[2]	0.10 ± 0.03	0.18 ± 0.04

as general nonlinear fitting functions to regress SPA 12 on solar forcing and CO_2. It is known that feed-forward ANNs with sufficiently enough free parameters can perform any arbitrary mapping of n-dimensional inputs to m-dimensional outputs [32]. We first prove here that ANNs can be advantageously used replacing standard linear statistical techniques, showing a better skill on this particular problem. To this end, we randomly selected 10% of the points in the whole SPA 12 record for testing purposes. The remaining data were randomly split in fractions of: (i) 80% used to iteratively adjust internal parameters by a gradient descent minimization of the output error, and (ii) 10% employed for monitoring and early stopping this process, i.e., before overfitting the data (we built ANNs consisting of 2 units in the input layer, 20 units in the second layer, and 1 unit in the output layer). Simultaneously, a linear model was adjusted and tested on exactly the same sets. This procedure was run in parallel for 200 different random partitions. The result of a paired t-test was 100% conclusive: irrespective of the temperature reconstruction considered, in all 200 cases an ANN explained more variance than a linear model. Average results and confidence limits are presented in Table 3.

Now the question naturally arises as to what the variance explained by each input in these nonlinear bivariate models is. Following the standard practice in nonlinear modeling, we alternatively eliminate the solar and CO_2 inputs off the ANN and measure the performance loss, repeating this process on the same 200 different random partitions considered above. In this way we obtained the individual contributions reported in Table 4.

We observe that nonlinear models employ more actively the CO_2 input than linear models do (contrast the $E.V._{CO_2}$ values against those in Table 2). To a lesser extent, the same conclusion also holds true for the solar driving. In particular, since the level of $E.V._{Sun}$ is the same, the response to solar variations in [2] seems to be essentially linear. Overall, a comparison among the results for $E.V._{Sun}$ in Table 4 reaffirms the contention that temperature variations in SPA 12 exhibit a stronger solar signature. We attribute this property to its extremely good age control with a better than decadal resolution, giving insight into temperature fluctuations wiped out by the stack character of other reconstructions.

References

[1] M.E. Mann, R.S. Bradley, M.K. Hughes, Global-scale temperature patterns and climate forcing over the past six centuries, Nature 392 (1998) 779–787.
[2] M.E. Mann, P.D. Jones, Global surface temperatures over the past two millenia, Geophys. Res. Lett. 30 (2003) 5-1–5-4.
[3] R.S. Bradley, M.K. Hughes, H.F. Diaz, Climate change: climate in medieval time, Science 302 (2003) 404–405.
[4] W.S. Broecker, Was the Medieval Warm Period global? Science 291 (2001) 1497–1499.
[5] A.F. Lotter, H.J.B. Birks, U. Eicher, W. Hofmann, J. Schwander, L. Wick, Younger Dryas and Allerod summer temperatures at Gerzensee (Switzerland) inferred from fossil pollen and cladoceran assemblages, Paleogeog. Paleoclimatol. Paleoecol. 159 (2000) 349–361.
[6] R.A. Muller, G.J. MacDonald, Glacial cycles and astronomical forcing, Science 277 (1997) 215–218.
[7] L.D. Keigwin, The Little Ice Age and Medieval Warm Period in the Sargasso Sea, Science 274 (1996) 1503–1508.
[8] H. Wanner, G. Dimitrios, J. Luterbacher, R. Rickli, E. Salvisberg, C. Schmutz, Klimawandel im Schweizer Alpenraum, VDF Hochschulverlag, Zürich, 2000, 285 pp.
[9] H. Holzhauser, Fluctuations of the Grosser Aletsch Glacier and the Gorner Glacier during the last 3200 years: new results, in: B. Frenzel (Ed.), Glacier Fluctuations During the Holocene, Fischer, Stuttgart, 1997, pp. 35–58.
[10] A. Moberg, D.M. Sonechkin, K. Holmgren, N.M. Datsenko, W. Karlen, Highly variable Northern Hemisphere temperatures reconstructed from low- and high-resolution proxy data, Nature 433 (2005) 613–617.
[11] C. Spötl, A. Mangini, S.J. Burns, N. Frank, R. Pavuza, Speleothems from high alpine Spannagel Cave, Zillertal Alps (Austria), in: I. Sasowsky, J. MyIroie (Eds.), Studies of Cave Sediments, Kluwer Academic, New York, 2004, pp. 243–256.
[12] N. Frank, M. Braun, U. Hambach, A. Mangini, G. Wagner, Warm period growth of travertine during the last interglaciation in southern Germany, Quat. Res. 54 (2000) 38–48.
[13] U. Neff, S.J. Burns, A. Mangini, M. Mudelsee, D. Fleitmann, A. Matter, Strong coherence between solar variability and the monsoon in Oman between 9 and 6 kyr ago, Nature 411 (2001) 290–293.
[14] C. Spötl, T. Vennemann, Continuous-flow IRMS analysis of carbonate minerals, Rapid Communications in Mass Spectrometry 17 (2003) 1004–1006.

[15] C.H. Hendy, The isotopic geochemistry of speleothems—I. The calculation of the effects of different modes of formation on the isotopic composition of speleothems and their applicability as palaeoclimatic indicators, Geochim. Cosmochim. Acta 35 (1971) 801–824.
[16] S.T. Kim, J.R. O'Neil, Equilibrium and nonequilibrium oxygen isotope effects in synthetic carbonates, Geochim. Cosmochim. Acta 61 (1997) 3461–3475.
[17] J. Luterbacher, D. Dietrich, E. Xoplaki, M. Grosjean, H. Wanner, European seasonal and annual temperature variability trends, and extremes since 1500, Science 303 (2004) 1499–1503.
[18] R.A. Muller, J.M. Gordon, Ice Ages and Astronomical Causes, Springer-Verlag, Berlin, 2000, 318 pp.
[19] C. Loehle, Climate change: detection an attribution of trends from long-term geologic data, Ecol. Model. 171 (2004) 433–450.
[20] G. Bond, B. Kromer, J. Beer, R. Muscheler, M.N. Evans, W. Showers, S. Hoffmann, R. Lotti-Bond, I. Hajdas, G. Bonani, Persistent solar influence on North Atlantic climate during the Holocene, Science 294 (2001) 2130–2136.
[21] W.S. Broecker, The Role of the Ocean in Climate Yesterday, Today and Tomorrow, ELDIGIO Press, Palisades, N.Y., 2004, 176 pp.
[22] S. Niggemann, A. Mangini, M. Mudelsee, D.K. Richter, G. Wurth, Sub-Milankovitch climatic cycles in Holocene stalagmites from Sauerland, Germany, Earth Planet. Sci. Lett. 216 (2003) 539–547.
[23] S. Niggemann, A. Mangini, D.K. Richter, G. Wurth, A paleoclimate record of the last 17,600 years in stalagmites from the B7-cave, Sauerland, Germany, Quat. Sci. Rev. 22 (2002) 555–567.
[24] Statistical treatment of environmental isotope date in precipitation, E. IAEA (Ed.), Tech. Rep. Ser., vol. 206, IAEA, 1981, 255 pp.
[25] D.W.J. Thompson, J.M. Wallace, Regional climate impacts of the Northern Hemisphere annular mode, Science 293 (2001) 85–89.
[26] J.M. Wallace, D.W.J. Thompson, Annular modes and climate prediction, Physics Today (2002) 28–33.
[27] H. Wanner, J. Luterbacher, C. Casty, R. Böhm, E. Xoplaki, Variabilität von Temperatur und Niederschlag in den europäischen Alpen seit 1500, in: F. Jeanneret, D. Wastl-Walter, U. Wiesmann, M. Schwyn (Eds.), Welt der Alpen- Gebirge der Welt, Haupt, Bern, 2003, pp. 61–76.
[28] A. Kaiser, H. Scheifinger, M. Kralik, W. Papesch, D. Rank, W. Stichler, Links between meteorological conditions and spatial/temporal variations in long-term isotopic records from the Austrian precipitation network, in: H. I.A.E.A. (Ed.), Study of Environmental change Using Isotope Techniques, C&S Paper Series 13/B, IAEA, Vienna, 2001, pp. 67–77.
[29] G. Humer, Niederschlagsisotopennetz Österreich: Daten, Umweltbundesamt Monogr 52, 1995, Vienna, 86 pp.
[30] M. Stuiver, T.F. Braziunas, Sun, ocean, climate and atmospheric $^{14}CO_2$: an evaluation of causal and spectral relationships, The Holocene 3 (1993) 289–305.
[31] D.M. Etheridge, L.P. Steele, R.L. Lagenfelds, R.J. Francey, J.M. Barnola, V.I. Morgan, Natural and anthropogenic changes in atmospheric CO_2 over the last 1000 years from air in Antartic ice and firn, J. Geophys. Res. 101 (1996) 4115–4128.
[32] G. Cybenko, Approximations by superpositions of a sigmoidal function, Math. Control Signal Systems 2 (1989) 303–314.